Eur. J. Biochem. **271**, 253–262 (2004) © FEBS 2003 doi:10.1046/j.1432-1033.2003.03923.x

Mutational and computational analysis of the role of conserved residues in the active site of a family 18 chitinase

Bjørnar Synstad[1], Sigrid Gåseidnes[1], Daan M. F. van Aalten[2], Gert Vriend[3], Jens E. Nielsen[4,*] and Vincent G. H. Eijsink[1]

[1]*Department of Chemistry and Biotechnology, Agricultural University of Norway, Ås, Norway;* [2]*Division of Molecular Microbiology and Biological Chemistry, Wellcome Trust Biocentre, University of Dundee, UK;* [3]*CMBI, University of Nijmegen, the Netherlands;* [4]*Howard Hughes Medical Institute & Department of Chemistry and Biochemistry, University of California San Diego, La Jolla, CA, USA*

Glycoside hydrolysis by retaining family 18 chitinases involves a catalytic acid (Glu) which is part of a conserved DXDXE sequence motif that spans strand four of a $(\beta\alpha)_8$ barrel (TIM barrel) structure. These glycoside hydrolases are unusual in that the positive charge emerging on the anomeric carbon after departure of the leaving group is stabilized by the substrate itself (the *N*-acetyl group of the distorted −1 sugar), rather than by a carboxylate group on the enzyme. We have studied seven conserved residues in the catalytic center of chitinase B from *Serratia marcescens*. Putative roles for these residues are proposed on the basis of the observed mutational effects, the pH-dependency of these effects, pK_a calculations and available structural information. The results indicate that the pK_a of the catalytic acid (Glu144) is 'cycled' during catalysis as a consequence of substrate-binding and release and, possibly, by a back and forth movement of Asp142 between Asp140 and Glu144. Rotation of Asp142 towards Glu144 also contributes to an essential distortion of the *N*-acetyl group of the −1 sugar. Two other conserved residues (Tyr10 and Ser93) are important because they stabilize the charge on Asp140 while Asp142 points towards Glu144. Asp215, lying opposite Glu144 on the other side of the scissile glycosidic bond, contributes to catalysis by promoting distortion of the −1 sugar and by increasing the pK_a of the catalytic acid. The hydroxyl group of Tyr214 makes a major contribution to the positioning of the *N*-acetyl group of the −1 sugar. Taken together, the results show that catalysis in family 18 chitinases depends on a relatively large number of (partly mobile) residues that interact with each other and the substrate.

Keywords: *Serratia marcescens*, electrostatics, pK_a, mutagenesis, pH optimum.

Chitin, a β-1,4-linked polymer of *N*-acetylglucosamine (GlcNAc), is degraded in nature by chitinases and β-*N*-1-4-acetylhexosaminidases (chitobiases). On the basis of sequence similarities, chitinases can be subdivided into two families (families 18 and 19) that differ in structure and mechanism [1]. Family 18 chitinases are retaining glycoside hydrolases that have been found in many organisms varying from bacteria to humans [1,2]. The catalytic domains of family 18 chitinases have a $(\beta\alpha)_8$ (TIM barrel) fold [3–8] and are characterized by several conserved sequence motifs [9,10]. The most prominent of these motifs is the DXDXE motif that spans strand 4 of the TIM barrel and includes the glutamate that acts as the catalytic acid. The active site grooves of these chitinases are lined with aromatic amino acids that contribute to substrate binding [6,11].

Catalysis in retaining glycoside hydrolases usually depends on at least two carboxylate side chains [12,13]. One of these provides acid/base assistance by first donating a proton to the leaving group and subsequently abstracting a proton from an incoming water molecule. The other carboxylate group functions as a nucleophile that stabilizes the oxocarbenium ion-like intermediate states by formation of a covalent glycosyl-enzyme intermediate [12–15]. Family 18 chitinases are unusual in that they lack a carboxylate that is properly positioned for acting as nucleophile. On the basis of studies on the family 18 chitinase hevamine [16], a family 20 chitobiase [17] and other *N*-acetylhexosaminidases [18], Tews *et al.* [19] proposed that catalysis in family 18 chitinases proceeds via formation of an oxazolinium ion. This intermediate is formed upon nucleophilic attack of the carbonyl oxygen of the *N*-acetyl group of the (distorted) −1 sugar on the anomeric carbon (Fig. 1). The results of further studies on hevamine [20] and chitinase B from *Serratia marcescens* (ChiB [21]), in addition to modelling studies [22], all support a mechanism that includes the formation of an oxazolinium ion. The proposed mechanism has been

Correspondence to V. Eijsink, Department of Chemistry and Biotechnology, Agricultural University of Norway, P.O. Box 5040, 1432 Ås, Norway.
Fax: + 47 6494 7720, Tel.: + 47 6494 9472,
E-mail: vincent.eijsink@ikb.nlh.no

Abbreviations: GlcNAc, 2-acetoamido-2-deoxy-D-glucopyranose (*N*-acetylglucosamine); $(GlcNAc)_n$, β-1,4-linked oligosaccharide of GlcNAc with a polymerization degree of n; 4-MU, 4-methylumbelliferyl.

Enzyme: chitinase B (Chi B) from *Serratia marcescens* (EC 3.2.1.14).

**Present address*: Department of Biochemistry, Conway Institute, University College Dublin, Ireland.

(Received 21 August 2003, revised 29 October 2003, accepted 12 November 2003)

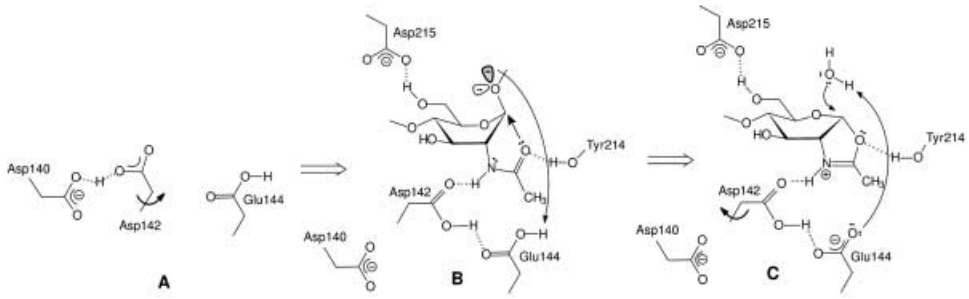

Fig. 1. Catalytic mechanism of family 18 chitinases. See text for details. Adapted from van Aalten *et al.* [21]. (A) Empty enzyme; (B) Binding and distortion of the substrate (the −1 sugar is shown), leaving group departure, and formation of the oxazolinium ion intermediate; (C) Hydrolysis of the oxazolinium ion intermediate. Copyright National Academy of Sciences, USA.

questioned on the basis of studies of chitinase A from *S. marcescens* [23], but convincing evidence for the formation of an oxazolium ion intermediate in β-*N*-1-4-acetylhexosaminidases has recently been described [24,25].

Although the overall sequence similarity between family 18 chitinases is not particularly high (average pairwise identity 21%; http://www.sanger.ac.uk/Software/Pfam), their active site regions contain many residues that are fully or highly conserved and whose (catalytic) functions are only partly understood (e.g. in ChiB: Tyr10, Ser93, Asp140, Asp142, Glu144, Tyr214, Asp215). Mutation of subsets of these conserved residues in various family 18 chitinases has shown for the majority that they are important for catalysis [20,26–31]. However, the mechanistic roles of several of these residues are not described well and there is no example of mutational analysis of all of these residues in the same enzyme.

To obtain an insight into how the many conserved residues in the active sites of family 18 chitinases contribute to catalysis, we have conducted a mutagenesis study of ChiB from *S. marcescens*, for which a wealth of structural information is available [6,21,32]. We employed a sensitive assay for enzyme activity, which permitted determination of pH-dependent activity of even the least active ChiB variants. We also conducted calculations of pK_a values of several residues in ChiB variants with and without bound substrate, using newly developed superior computational methods [33,34]. The results were interpreted with the use of available structural information and used to propose roles for the mutated residues during the catalytic cycle.

Materials and methods

Genetic techniques

Prior to site-directed mutagenesis, fragments of the *chiB* gene (from plasmid pMAY2-10 [21]) were subcloned into plasmids pGEM5Z(+) or pGEM3Z(+) (Promega, Madison, WI, USA). Mutagenesis was performed using the QuikChange™ Site-directed Mutagenesis Kit from Stratagene (La Jolla, CA, USA) essentially as described by the manufacturer. Sequences of mutated *chiB* fragments were verified using the ABI PRISM™ Dye Terminator Cycle Sequencing Ready Reaction Kit and an ABI PRISM 377 DNA Sequencer (PerkinElmer Applied Biosystem, Foster City, CA, USA). Fragments with the correct sequence were used to construct variants of pMAY2-10 containing an intact *chiB* gene with the desired mutation. pMAY2-10 variants were transformed into competent *Escherichia coli* DH5α™ (Life Technologies, Rockville, MD, USA) and the resulting strains were used for enzyme production. Bacteria were grown in Luria–Bertani medium supplemented with 50 μg·mL^{-1} ampicillin. For plates, the medium was solidified with 1.5% (w/v) agar.

Production and purification of wildtype and mutated ChiB

ChiB variants were purified from periplasmatic extracts of the producer strains by hydrophobic interaction chromatography, as described previously [35]. Columns were washed extensively between purifications to prevent cross-contamination of low activity mutants. Lack of cross-contamination was indicated by the fact that active site mutants with severely impaired activity showed pH-activity profiles that differed dramatically from the pH-activity profile recorded for wildtype enzyme purified in a preceding run. Enzyme purity was verified using SDS/PAGE. Protein concentrations were determined using the Bradford assay kit provided by Bio-Rad (Hercules, CA, USA).

Enzyme assays

The activity of ChiB variants was determined using the $(GlcNAc)_3$ analogue 4-methylumbelliferyl-β-D-*N*-*N*′-diacetylchitobioside [4-MU-$(GlcNAc)_2$] as substrate. Enzyme concentrations were adapted to the varying activities of the ChiB variants. In a standard assay, 100 μL of a mixture containing enzyme, 20 μM substrate, 50 mM citrate/phosphate buffer, pH 6.3 [36] and 0.1 mg·mL^{-1} bovine serum albumin was incubated at 37 °C for 10 min, after which the reaction was stopped by adding 1.9 mL of 0.2 M Na_2CO_3. The amount of 4-methylumbelliferyl (4-MU) released was determined using a DyNA 200 Fluorimeter (Hoefer Pharmacia Biotech, San Francisco, CA, USA).

Specific activities were determined using a relatively low substrate concentration of 20 μM to avoid effects of substrate inhibition [35]; this means that changes in specific activities may to some extent reflect changes in K_m. Kinetic parameters were determined by initial rate measurements using substrate concentrations in the 5–40 μM range. Linearity was ensured by monitoring product formation

at four time points for each reaction (product formation was linear for at least 20 min, at all substrate concentrations, at almost all pH values and for all mutants). In this way kinetic parameters could be determined with sufficient accuracy despite the narrow range of substrate concentrations. K_m and k_{cat} values were determined using hyperbolic regression with the program HYPER (J. S. Easterby, University of Liverpool, UK; obtainable from the website http://www.liv.ac.uk/~jse/software.html). For each ChiB variant at each pH, K_m and k_{cat} values were determined three times in independent experiments. The values presented below are average values derived from these three independent experiments. At pH values below 4.2 and above 9.0–10.0 (8.0 for the Y10F mutant), enzyme instability precluded accurate analysis of catalytic properties.

Variation in pH was achieved by replacing 50 mM citrate/phosphate buffer, pH 6.3, in the assay mixture with other buffers with appropriate pH (all at 50 mM concentration). Several buffer types were tested, which resulted in selection of a set of buffers whose constituents did not significantly affect enzyme activity. The following buffers were used: pH 4.2, 4.6, 5.0, 5.4, 6.3 and 6.6 citrate/phosphate buffer, pH 7.2 sodium phosphate buffer, pH 8.0, 8.3 and 9.0 bicine/HCl buffer and pH 9.0, 9.5 and 10.0 ethanolamine/HCl buffer [36].

Structural analysis and electrostatics calculations

Studies of chitinase structures and molecular modelling were performed with WHAT IF software [37]. pK_a calculations were carried out with the WHAT IF pK_a calculation package [33,34,38]. A dielectric constant of 80 was used for the solvent, and a dielectric constant of eight was used for the protein [39]. A significant speed-up of the calculations was achieved by calculating pK_a values for only a subset of the titratable groups in the protein. The subset of titratable groups was selected by applying a two-step selection procedure as described in [34]. Briefly, groups interacting strongly (interaction energy > 1.0 kT·e^{-1}) with either Asp140, Asp142, Glu144 or Asp215 were defined as the 'first shell'. Additionally, groups interacting strongly (interaction energy > 2.0 kT·e^{-1}) with groups in the first shell were defined as the 'second shell'. All residues in the first and second shell, as well as Asp140, Asp142, Glu144 and Asp215 were included fully in the calculation, whereas all other groups were treated less rigorously. This approach provides huge savings in calculation time and has been shown to give accurate results [34]. The identity of the groups that are included fully in the calculation is listed on the http://enzyme.ucd.ie/pKa/chitinase/ website. This website also provides access to all calculated titration curves.

Point mutations were also modelled using WHAT IF [37]. The character of the mutations was such that steric effects on the surrounding residues were expected to be minimal; consequently we altered only the coordinates for the mutated residue. In all cases we utilized the WHAT IF position-specific rotamer library [40] to check that the rotamer distributions of the original and mutant residue were compatible.

Figure 2 was prepared using PYMOL software [41].

Results and discussion

Figure 2 shows part of the structure of ChiB, highlighting the residues discussed in this report. In the free enzyme, Asp142 is in the 'down' position, interacting with Asp140. Upon substrate-binding, Asp142 moves into the 'up' position and interacts with the substrate and Glu144. This rotation of Asp142 is accompanied by removal of a water molecule and adjustments of Tyr10 and Ser93 that seem to compensate Asp140 for the loss of its hydrogen bonding partner (discussed previously in [21]). Asp215 and Tyr214 both interact with the substrate. The smallest distance between the oxygen in the scissile glycosidic bond and Asp140 is 10.7 Å.

Mutational effects

The residues mutated in this study are shown in Fig. 2. Asp140, Asp142, Glu144 and Asp215 were mutated individually to asparagine and alanine, Tyr10 and Tyr214 were replaced by Phe, and Ser93 was replaced by alanine. All clones expressing ChiB variants yielded wildtype-like amounts of protein, with the exception of Y10F, which yielded approximately 10 times less protein.

The enzymatic activities of the mutant proteins were analyzed by measuring specific activity at pH 6.3 (Table 1), as well as by determining K_m and k_{cat} at various pH values (Table 2; Fig. 3). The acidic limb of the pH-activity profiles could not be determined as the enzyme is unstable at low pH.

To check for possible artefacts caused by cross-contamination during mutant purification or by deamidation in the D140N, D142N, E144Q and D215N mutants, the pH-dependency of specific activity was recorded for these four mutants and the four corresponding alanine mutants. The least active mutants (i.e. the alanine mutants) were deliberately purified using a column (washed with our standard protocol) that had been used for purification of wildtype enzyme in the preceding run. Some of the pH profiles differed strongly from the wildtype profile, however, the profiles for the amide and corresponding alanine mutants were similar in all cases. Together these observations show that it is unlikely that the low activities recorded for some of the mutants discussed in this report are due to cross-contamination or deamidation. We can, however, not exclude this possibility for the E144Q mutant as this mutant displayed a similar pH-activity profile to the wildtype (discussed below).

Table 1 shows that all mutations reduced the specific activity at pH 6.3. Mutation of the catalytic Glu yielded the largest reduction in activity ($1 \times 10^4 - 1 \times 10^5$ -fold) with E144A being about one order of magnitude less active than E144Q. Of the Asp $\rightarrow$ Xxx mutants, D142N and D215N mutants continued to display considerable activity (3–5% of wildtype activity) whereas the activities of the cognate alanine mutants were greatly reduced ($1 \times 10^3 - 1 \times 10^4$-fold). Mutation of Asp140 resulted in a 1×10^3-fold decrease in activity regardless of whether alanine or asparagine was introduced. Another deleterious mutation was Y214F, which reduced specific activity by two orders of magnitude. Mutation of Tyr10 or Ser93 decreased specific activity approximately 20-fold.

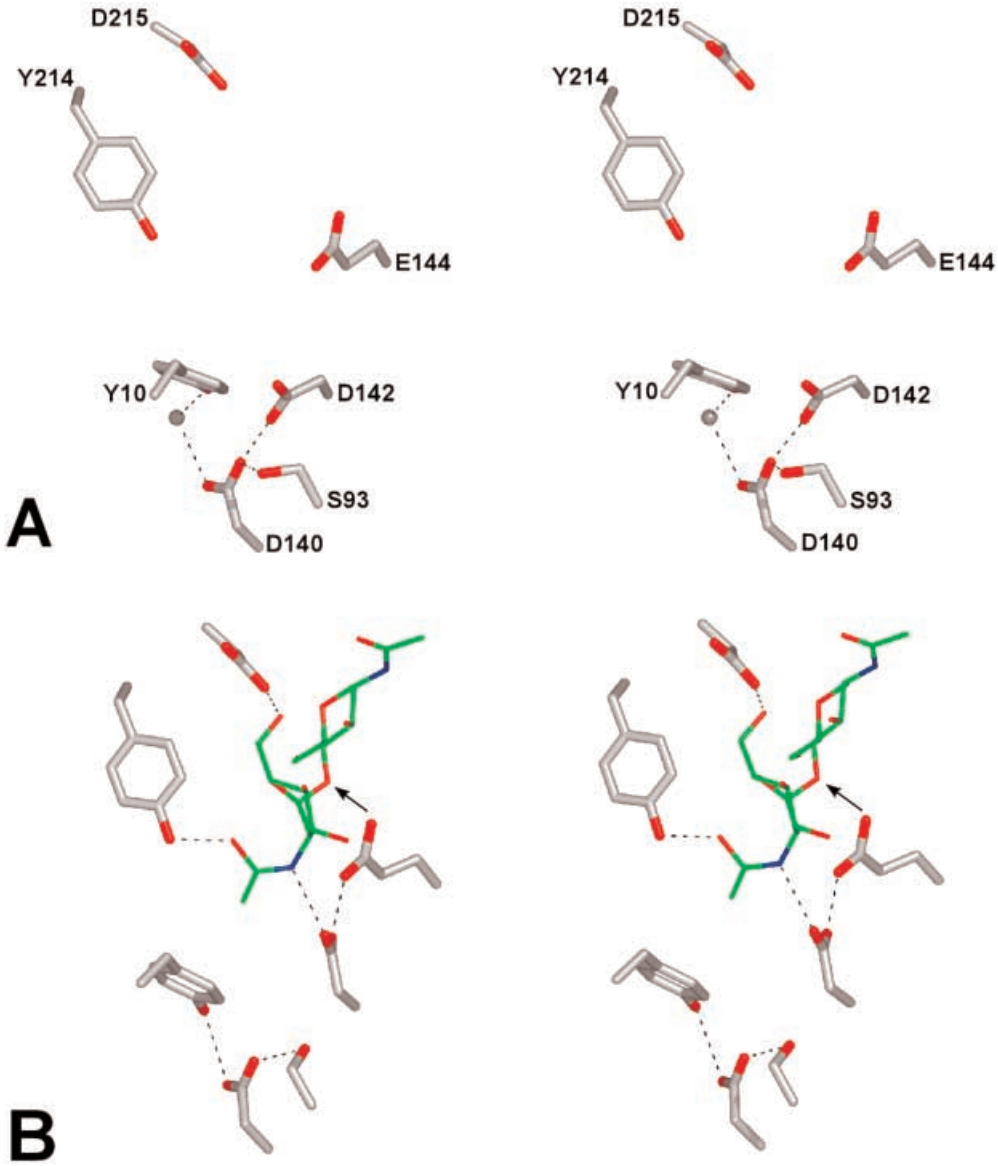

Fig. 2. Overview of residues mutated in ChiB. The figure shows stereo images of (A) substrate-free wildtype ChiB (PDB accession code 1E15) and (B) the E144Q mutant of ChiB in complex with $(GlcNAc)_5$ (PDB accession code 1E6N). Gln144 has been mutated back to Glu144 for illustration purposes. For clarity only two of the five GlcNAc moieties are shown (bound to subsites −1 and +1). Carbon atoms in the bound sugar are green. Hatched lines indicate hydrogen bonds. The arrow in (B) points from the catalytic glutamate to the glycosidic oxygen. Note that the water molecule depicted as a grey sphere in (A) is only present in the free enzyme. See text for details.

Several of the mutations had clear effects on the pH-dependency of k_{cat} and k_{cat}/K_m (Fig. 3). K_m values were almost independent of pH in the 4.2–9.0 range, whereas a slight increase (factor 2–3) was observed at pH 10.0 (for mutants that were still active and measurable at this pH). Mutational effects on K_m were small (less than a factor of two), with the exception of D142N. The latter mutant displayed a four to tenfold reduction in K_m in the pH 4.2–8.0 range, and a marked increase in K_m at alkaline pH (Table 2, Fig. 3).

The D215N and D140N mutants displayed an acidic shift in the pH-activity profiles, whereas the Y214F and the E144Q mutants showed wildtype-like profiles (Fig. 3). Interesting mutational effects were observed for the D142N and S93A mutants, whose k_{cat} values were almost independent of pH over the entire tested range (Fig. 3A). In addition, these two mutants are the only ChiB variants that show a clear difference between their k_{cat} and k_{cat}/K_m profiles, the latter being more wildtype-like in shape (Fig. 3B). At alkaline pH, the k_{cat}/K_m curves of the D142N and S93A mutants almost merge with that of the wildtype. At lower pH, the two mutants have considerably lower k_{cat}/K_m values than the wildtype (Fig. 3B; Table 2).

Due to stability problems, the catalytic properties of Y10F could not be measured in the alkaline pH-range.

Table 1. Specific activity of ChiB variants at pH 6.3. WT, wildtype.

Variant	Specific activity	
	$nmol \cdot s^{-1} \cdot mg^{-1}$	% of WT
Y10F	7.9 ± 0.5	5.7
S93A	7.7 ± 0.4	5.6
D140N	0.17 ± 0.04	0.12
D140A	0.17 ± 0.01	0.12
D142N	4.4 ± 0.5	3.2
D142A	0.13 ± 0.01	0.094
E144Q	0.028 ± 0.015	0.023
E144A	0.0016 ± 0.0003	0.0012
Y214F	1.04 ± 0.06	0.75
D215N	5.8 ± 0.7	4.2
D215A	0.043 ± 0.001	0.031
WT	138 ± 22	100

pK_a calculations

pK_a values for Asp140, Asp142, Glu144 and Asp215 were calculated in several ChiB mutants as described in Materials and methods (Table 3). Calculations were primarily based on the X-ray structures of ligand-free wildtype ChiB (PDB accession code 1E15 [9]); and on the structure of the E144Q mutant with $(GlcNAc)_5$ bound to subsites −2 to +3 (PDB accession code 1E6N [21]). Prior to some of the calculations one or more adjustments were made to the structures, as listed in Table 3. Results for Asp215 were omitted from Table 3, as the calculated pK_a for this residue was below 1.0 in all situations. The presence of a strong salt bridge with Arg294 (not shown; closest contact 2.3 Å, Asp215-Oδ1 and Arg294-Nη1) provides an explanation for the low pK_a value for Asp215.

Previous studies have shown that the software used for pK_a calculations in this study can yield accurate and useful results [34,38,39], particularly for glycoside hydrolases [39,42]. On the other hand these methods do not, or only partly, account for several important complexities, e.g. relation to dynamics, desolvation effects and transient charges (Nielsen & McCammon [34] provide a discussion on the accuracy of this type of calculation). In the present case, an additional complexity comes from the fact that catalysis seems to rely on the interplay between at least four titratable groups (residues 140, 142, 144 and 215). Moreover, pK_a calculations are sensitive to minor structural changes [34], meaning that comparisons of values derived from different crystal structures are inherently inaccurate. Because of these complexities, it is not appropriate to compare the calculated pK_a values (some of which are quite extreme in the present study) directly with the apparent pK_a values that can, in principle, be derived from the pH-activity curves presented in Fig. 3. The calculations can, however, be used to qualitatively analyze the effects of site-directed mutations, substrate-binding and structural adjustments, as such analysis does not rely on absolute pK_a values and may be based on comparisons of almost identical structures.

The calculations strongly suggest that the Asp140-Asp142 pair in the wildtype enzyme carries precisely one negative charge over the whole experimentally accessible pH range, regardless of the position of Asp142 (pK_a values are < 0.0 and 15.2 to > 20.0; Table 3, rows 1, 5–8). The pK_a of Asp140 is much lower than that of Asp142 and Glu144 in all situations where all three residues are present and the one proton shared by Asp140 and Asp142 appears to remain on Asp142 when this residue moves to the 'up' position. Previous structural studies support this result: when Asp142 rotates 'up', Tyr10 and Ser93 move towards Asp140, donating hydrogen bonds to the carboxylic group that is consequently likely to be ionized ([21]; Fig. 2). The calculated pK_a values for Glu144 in the wildtype enzyme varied from 7.1 to 12.5, indicating that this residue is protonated at pH values where the enzyme is most active. Summarizing, the calculations show that the carboxylic groups in the Asp140-Asp142-Glu144 triad contain two protons at the pH where the enzyme is most active. The basic arm of the pH-activity profile must be determined by the loss of one or both of these protons.

Comparison of rows 1, 6 and 8 with rows 5 and 7 in Table 3 shows that substrate-binding has drastic effects on the pK_a of Glu144, raising it by 3.8 to 5.4 units, depending on the position of Asp142 and the calculation used. Interestingly, the calculations also suggest that the magnitude of this effect is in part due to the presence of the negatively charged Asp215 (whose side chain is close to the glycosidic oxygen): comparison of rows 4 and 11 shows that the calculated effect of substrate-binding on the pK_a of Glu144 is only 2.3 in the D215N mutant. Evaluation of

Table 2. Kinetic parameters at pH 4.2, 6.3 and 9.0. pH activity profiles are presented in Fig. 3. WT, wildtype; ND, not determined.

Variant	k_{cat} (s^{-1})			K_m (μM)		
	pH 4.2	pH 6.3	pH 9.0	pH 4.2	pH 6.3	pH 9.0
WT	13.1 ± 2.3	17.8 ± 2.3	1.2 ± 0.3	31.1 ± 8.2	30.9 ± 6.3	45.6 ± 14.4
Y10F	1.55 ± 0.25	1.4 ± 0.27	–[a]	53.5 ± 11.1	43.2 ± 10.8	–[a]
S93A	0.45 ± 0.05	0.59 ± 0.08	0.29 ± 0.04	23.8 ± 3.9	25.4 ± 5.0	40.4 ± 7.6
D140N	0.53 ± 0.05	0.026 ± 0.006	ND	54.9 ± 7.1	51.6 ± 14.9	ND
D142N	0.26 ± 0.07	0.28 ± 0.04	0.31 ± 0.05	5.4 ± 1.2	4.1 ± 2.0	16.6 ± 5.3
E144Q	0.0039 ± 0.0007	0.0043 ± 0.0005	0.001 ± 0.0002	14.7 ± 5.4	19.1 ± 4.2	13.4 ± 4.2
Y214F	0.117 ± 0.014	0.117 ± 0.011	0.016 ± 0.002	37.3 ± 7.9	20.2 ± 4.3	97 ± 14.7
D215N	3.26 ± 0.63	0.76 ± 0.2	0.023 ± 0.007	48.7 ± 12.1	33.2 ± 13.5	87.3 ± 30.1

[a] The kinetic parameters of Y10F could not be measured at pH 9.0 due to enzyme instability. At pH 8.0 Y10F showed a k_{cat} of 0.55 and K_m of 47.2 (compared to a k_{cat} of 3.5 and a K_m of 24.9 in the wildtype at pH 8.0).

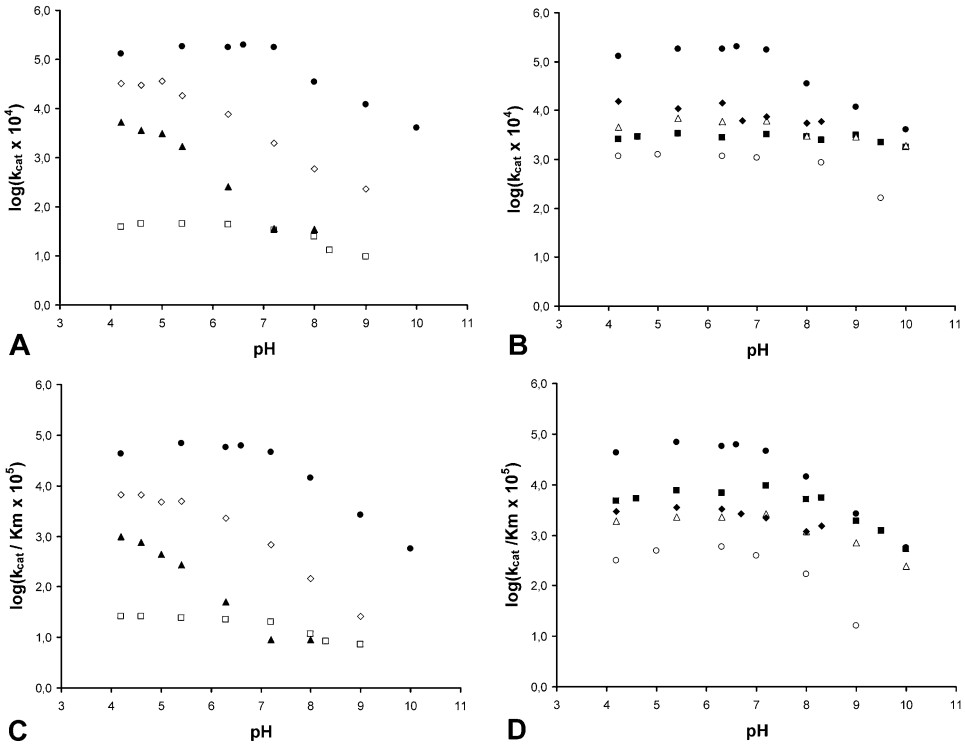

Fig. 3. Kinetic analysis. (A) and (B) The effect of pH on k_{cat} (s^{-1}), and (C) and (D) k_{cat}/K_m ($s^{-1}\cdot\mu M^{-1}$), on the hydrolysis of 4-MU-$(GlcNAc)_2$ at 37 °C. The ChiB variants shown are wildtype, ●; D215N, ◇; D140N, ▲; E144Q, □; Y10F, ◆; S93A, △; D142N, ■ and Y214F, ○. Note that the points for D142N and wildtype overlap at high pH in (D).

Table 3. Calculated p*K*a values. Details, titration curves and more calculations may be found on http://enzyme.ucd.ie/pKa/chitinase/. 1E15 is the crystal structure of the free wildtype enzyme; 1E6N is the crystal structure of the E144Q mutant in complex with $(GlcNAc)_5$. WT, wildtype.

Number of calculation	Structure	Modelled adjustments	Mutation compared to wildtype enzyme	Calculated p*K*a values		
				Asp140	Asp142	Glu144
1	1E15		WT	< 0.0[a]	> 20.0[a]	7.1
2	1GOI[b]	D140N	Absent	11.3	8.4	
3	1E15[c]	D142N, Asn142 'up'[c]	D142N	< 0.0	Absent	6.7
4	1E15	D215N	D215N	< 0.0	12.4	5.7
5	1E6N	Q144E	WT	< 0.0	> 20.0	11.7
6	1E6N	Q144E, no substrate	WT	< 0.0	15.2	7.9
7	1E6N	Q144E, Asp142 'down'	WT	< 0.0[a]	> 20.0[a]	12.5
8	1E6N	Q144E, no substrate, Asp142 'down'	WT	< 0.0[a]	> 20.0[a]	7.7
9	1E6N	Q144E, D140N	D140N	Absent	7.7	14.9
10	1E6N	Q144E, D142N	D142N	5.0	Absent	9.7
11	1E6N	Q144E, D215N	D215N	< 0.0	> 20.0	8.0

[a] Calculations on structures in which Asp140 and Asp142 form a hydrogen bond (Asp142 in the 'down' position) in some cases yielded irregular titration curves indicating that one proton was alternating between the two residues. This prevented determination of individual pK_a values. Addition of the two titration curves yielded a flat line at charge −1, showing that the coupled Asp140-Asp142 system contains one proton at all pH values. For simplicity, and in line with the results from the other calculations, the < 0.0 value is allocated to Asp140 and > 20.0 to Asp142. [b] The calculations were performed on the crystal structure of the Dl40N mutant (PDB accession code 1GOI [31]). The structure shows Asp142 in the 'up' position. [c] Crystallographic results (G. Kolstad, unpublished observations) indicate that Asn142 in the D142N mutant is in the 'up' position. Therefore, residue 142 was positioned in the 'up' position.

rows 5 and 7 shows that in the presence of the substrate, rotation of Asp142 towards Glu144 lowers the pK_a of the latter by 0.8 pH units.

The calculated effects of the D140N and D215N mutations varied drastically between the various situations, but all calculations showed a clear reduction in the combined

pK_a of Asp142 and Glu144 (which is in accordance with the observed large acidic shifts in the pH-activity profiles).

The D142N mutation did not yield noticeable effects on pK_a values in the free enzyme. However, in the enzyme–substrate complex this mutation yielded several changes, including a potentially significant decrease in the pK_a of Glu144 (from 11.7 to 9.7; Table 3, rows 5 and 10).

Roles of conserved residues in the catalytic mechanism deduced from experimental and computational data

According to the calculations for the wildtype enzyme, Glu144 is the only relevant titratable residue in the pH 6–12 range and the pK_a of this residue is affected by substrate-binding. Therefore, it is surprising that the pH-k_{cat} profiles (where apparent pK_a values are likely to reflect pK_a values in the enzyme–substrate complex [43]) and pH-k_{cat}/K_m profiles (where apparent pK_a values are likely to reflect pK_a values in the apo-enzyme), are similar in the wildtype enzyme and in most mutants. It thus seems that the assumptions underlying this interpretation of the two different pH-activity plots [43] do not generally apply in the present system. One plausible cause for this is the strong degree of interaction and mobility in the Asp140-Asp142-Glu144 triad. Thus, the pH-activity curves are determined by simultaneous titrations of several interacting groups. Interestingly, the D142N mutant, which lacks a 'titratable' connection between residue 140 and 144, shows obviously different pH-k_{cat} and pH-k_{cat}/K_m profiles.

Glu144 and Asp142

The importance of Glu144 for catalysis is illustrated by the large reduction in enzyme activity upon mutation to glutamate or alanine that was observed in this study and previous studies on other family 18 chitinases [20,26,28–30]. Mutation of this residue to aspartate in other family 18 chitinases also reduced activity dramatically [26,29]. The pK_a calculations indicate that Glu144 has a slightly elevated pK_a in the free enzyme that, at least in part, results from the vicinity of Asp215 (Table 3, rows 1 and 4). The calculations indicate that the pK_a of Glu144 is further, and somewhat drastically, increased upon substrate-binding.

The D142N mutant is interesting because it retains significant activity (suggesting that a wildtype-like catalytic mechanism still applies) while displaying clear changes in the pH-activity profiles. Structural studies have shown that residue 142 makes an important contribution to distortion of the −1 sugar, in particular distortion of the *N*-acetyl group (Figs 1 and 2). Hydrogen bonds provided by an asparagine can to a large extent replace the hydrogen bonds made by aspartate, which may explain why the D142N mutant retains considerable activity, whereas the D142A mutant does not. It has been shown by X-ray crystallography that replacement of the Asp142 analogue by alanine in other family 18 chitinases puts the *N*-acetyl group in a conformation which is not favourable for nucleophilic attack on the anomeric carbon [20,23]. It is important to note that the D142A mutation is highly deleterious for catalytic activity (Table 1), thereby confirming the crucial role of Asp142.

In most ChiB structures, Asp142 is clearly defined, being either in the 'down' or in the 'up' position. A high-resolution structure of another family 18 chitinase from *S. marcescens* (ChiA [44]) shows that in this apoenzyme the analogue of Asp142 occupies both conformations. The Asp142 equivalent in the family 18 chitinase from *Coccidioides immitis* was found to be in the 'down' position in the apoenzyme and in the 'up' position in the complex with allosamidin [45], which is analogous to what was found for ChiB [21]. Crystal structures of ChiB-E144Q in complex with $(GlcNAc)_5$ and of wildtype ChiB in complex with the reaction intermediate analogue allosamidin [21], show that there is no room for Asp142 to rotate back and forth once the substrate is bound. So, rotation of Asp142 towards the substrate must happen concomitantly with substrate-binding and substrate-distortion. The pK_a calculations indicate that the proton shared by Asp140 and Asp142 in the apoenzyme remains on Asp142 when this residue moves to a position close to Glu144. It is conceivable that the presence of the protonated Asp142 close to Glu144 increases the acidity of the proton on Glu144, which again would lead to improved assistance to leaving group departure. Indeed, the pK_a calculations (Table 3, rows 5 and 7) indicate that rotation of Asp142 to the 'up' position lowers the pK_a of Glu144 (by 0.8 units). Such an effect of Asp142 is likely to be augmented during catalysis when Asp142 can pull electrons from Glu144 towards the developing positive charge of what will become the oxazolinium ion intermediate (Fig. 1C). Replacing Asp142 by a less polarizable asparagine would reduce this electron pulling ability.

It should be noted that the pK_a calculations do not apply to the situation during actual catalysis (i.e. with partial charges being formed, and covalent bonds being formed and broken). Thus, the calculated effect of rotation of Asp142 on the pK_a of Glu144 only gives an indication of what may happen to the acidity of Glu144. Although this calculated effect is small (0.8 units), it is likely to be significant as it is derived from structures that are identical except for the position of residue 142 [34].

The pK_a calculations indicate that the only candidate for a residue determining the basic arm of the pH-activity profile of the D142N mutant is Glu144. The pH-k_{cat}/K_m profiles show that the D142N mutant has wildtype-like activity at the highest pH values that were tested. The pH-k_{cat} profile shows a similar effect, but the two curves merge at considerably higher pH (Fig. 3). An appealing explanation for these observations is that Glu144 is ionized at the pH values where the wildtype and D142N curves merge, meaning that the effect of residue 142 on the acidity of the proton of Glu144 becomes less relevant. The fact that the wildtype and mutant curves merge at higher pH in the pH-k_{cat} plot would then be in accordance with the prediction that substrate-binding raises the pK_a of Glu144.

Tyr10 and Ser93

To our knowledge, there are no other mutational data in the literature that address the role of Tyr10 for catalysis. The importance of Ser93 has previously been shown (but not explained) in two mutational studies [26,28].

Structural studies [21] have shown that the rotation of Asp142 is accompanied by adjustment of Ser93 and Tyr10

which lead to a changed hydrogen bonding network around Asp140: (a) Tyr10 moves towards Asp140 thus replacing a water molecule that acts as a hydrogen bond donor in the apoenzyme, by a more acidic phenolic hydroxyl group, (b) the side chain of Ser93 rotates (by −114° around χ_1) which leads to relocation of the Ser93-Asp140 hydrogen bond and (c) the adjustments of Tyr10 and Ser93 partially fill the cavity left behind by Asp142. A similar structural adjustment is visible when comparing the structures of a *C. immitis* chitinase with and without allosamidin bound into the active site (PDB accession codes 1D2K and 1LL4 [45]).

The effects of mutating Ser93 and Tyr10 are similar to the effects of the D142N mutation. All three mutants had similar residual activities and pH-activity profiles. S93A displays a similar difference between the pH-k_{cat} and pH-k_{cat}/K_m profile as D142N. Together, these observations indicate that the functionality of Asp142 during catalysis depends on the presence of Ser93 and Tyr10.

Asp140

The D140N and D140A mutations had equally drastic reducing effects on the activity of ChiB, showing that the presence of an acidic residue at this position is essential. The pH-optimum shows an acidic shift, indicating that the D140N mutation lowers the pK_a of key catalytic residues. This is confirmed by the pK_a calculations, which show that the D140N mutation reduces the joint pK_as of Asp142 and Glu144. The primary role of Asp140 therefore seems to consist of providing a negative charge which keeps Asp142-Glu144 protonated.

The pK_a calculations yielded very low pK_a values for Asp140, which is remarkable taking into account the partly buried position of this residue. Of the three major environmental factors that are taken into account in the calculations (background charges, desolvation penalty and the interaction with other titratable residues), the first factor was found to be the major determinant of the acidity of Asp140. Thus, it would seem that the acidity of Asp140 is influenced by additional residues in ChiB, i.e. by the many positive residues further down in the TIM barrel (e.g. Lys82, Arg89, Arg174, Lys132 [6]). Further studies addressing this issue are currently in progress.

Asp215

It has been shown that distortion of the −1 sugar ring into a 4-sofa conformation is an inherent part of the catalytic mechanism (Fig. 1 [17,19,21,22]). Structural studies show that Asp142, Tyr214 and Asp215 are involved in binding the −1 sugar in a distorted boat conformation [21]. While Asp142 and Tyr214 primarily interact with the *N*-acetyl group of the −1 sugar (see also [20]), Asp215 stabilizes the observed boat conformation by accepting a hydrogen bond from the O6 hydroxy (Fig. 2). Asparagine is also able to fulfil this role, explaining the residual activity of the D215N mutant. The possibility to interact is obviously lost in the D215A mutant which in fact is one of the least active mutants described in this report.

The acidic shift in the pH-optimum of the D215N mutant shows that Asp215 has a second major role in catalysis, namely to increase pK_a values in the Asp142-Glu144 system. This role is confirmed by the pK_a calculations.

Tyr214

The ChiB–NAG_5 complex structure shows that Tyr214 interacts with the distorted *N*-acetyl group of the −1 sugar (Fig. 2B). Previous enzymological and structural studies of the effect of mutations analogous to Y214F (e.g. Y390F in ChiA from *S. marcescens* [23] and Y183F in hevamine [20]), have shown that this mutation reduces activity and that the only structural effect is a loss of the interaction between the hydroxyl group and the *N*-acetyl group. Our mutational results confirm that this residue is essential for catalytic efficiency. The hydroxyl group of Tyr214 does not interact with any of the carboxylic side chains in the catalytic center and accordingly, the Y214F mutant had similar pH-activity profiles as the wildtype.

Y214F affects k_{cat} but not K_m despite the apparently favourable interaction with the substrate (Fig. 2; the hydrogen bond with the substrate has a poor geometry). It has previously been shown that the Y214F mutation increases the affinity of ChiB for allosamidin, which is an analogue of the proposed oxazolinium ion intermediate [32]. The minor (or even positive) effects of Y214F on substrate and intermediate binding and the large negative effect on k_{cat} suggest that the hydroxyl group on Tyr214 is important for transitional state stabilization only.

Concluding remarks

The data reported from previous mutagenesis studies of subsets of these active site residues in family 18 chitinases [20,23,26–30] are generally in qualitative agreement with the results presented here. There are quantitative differences between the reported results, which may be due to differences in experimental conditions (e.g. substrates, pH) or to genuine differences between the enzymes. The most prominent difference is with regard to the role of Asp140, which appears to be crucial in ChiB and in chitinase A1 from *Bacillus circulans,* whereas it may be mutated to asparagine without loss of activity in other family 18 chitinases [28,30]. Preliminary results of a comparative study of available structures of family 18 chitinases and their complexes [8,20,21,23,44,45] show subtle variations in the polar cores of the TIM barrels near residue 140, which could account for the experimentally observed differences. It should also be noted that naturally occurring family 18 chitinases display different pH-optima.

The present results show that protonation of the catalytic glutamate is promoted by substrate-binding. In other words, it is the substrate itself that ensures that this glutamate is protonated, even at slightly basic pH. The experimentally observed and calculated effects of the D215N mutation show that the pK_a-raising effect of substrate-binding is partly due to the substrate's ability to conduct the negative charge on Asp215 to Glu144. Interestingly, hevamine and several other naturally occurring family 18 chitinases with clearly acidic pH-optima (around 4.2 [20,46]), have asparagine at the position analogous to Asp215 in ChiB. The D215N mutant of ChiB is in fact a

quite active 'acidic' chitinase with a pH optimum below pH 5.0.

Efficient catalysis requires 'cycling' of the pK_a of Glu144 (see also [47]). Initially this residue needs to be protonated, but subsequently it needs to make this proton acidic to promote leaving group departure. As explained above, it is conceivable that rotation of protonated Asp142 may contribute to a necessary lowering of the pK_a of Glu144 in the enzyme–substrate complex. Residue 142 has a complex function in catalysis as it also contributes to distortion of the substrate and to stabilization of the emerging positive charge (Fig. 1). Some of these roles can also be performed by an asparagine residue, but not by alanine (hence the very low activity of the D142A mutant).

The present study shows how catalysis in ChiB depends on the concerted action of at least seven conserved residues. Several of these residues are located relatively far from the scissile bond, for example the closest distances between the glycosidic oxygen in the scissile bond and the polar side chain atoms of Tyr10, Ser93 and Asp140 are 9.7 Å, 10.2 Å and 10.7 Å respectively. The presence of triads analogous to the Asp140-Asp142-Glu144 triads in glycoside hydrolases is not unique [42,48] but the present study extends this by showing how the functionality of such a triad is affected by the surrounding residues. The results so far indicate that larger parts of the polar core of the catalytic TIM barrel of family 18 chitinases play a role during catalysis. It will thus be interesting to see if other important residues are revealed by additional mutagenesis studies, for example of residues further down in the core of the TIM barrel.

Acknowledgements

This work was supported by the European Union, grant no. BIO4-CT-960670 and by the Norwegian Research Council, grant nos. 122004/112 and 140440/130. We thank Gustav Kolstad for helpful discussions and assistance with producing some of the illustrations, and Xiaohong Jia for skillful technical assistance. J.E.N. acknowledges support from the Howard Hughes Medical Institute and from the Danish Natural Research Science Council.

References

1. Henrissat, B. & Davies, G. (1997) Structural and sequence-based classification of glycoside hydrolases. *Curr. Opin. Struct. Biol.* **7**, 637–644.
2. Armand, S., Tomita, H., Heyraud, A., Gey, C., Watanabe, T. & Henrissat, B. (1994) Stereochemical course of the hydrolysis reaction catalyzed by chitinases A1 and D from *Bacillus circulans* WL-12. *FEBS Lett.* **343**, 177–180.
3. Perrakis, A., Tews, I., Dauter, Z., Oppenheim, A.B., Chet, I., Wilson, K.S. & Vorgias, C.E. (1994) Crystal structure of a bacterial chitinase at 2.3 Å resolution. *Structure* **2**, 1169–1180.
4. Terwisscha van Scheltinga, A.C., Kalk, K.H., Beintema, J.J. & Dijkstra, B.W. (1994) Crystal structures of hevamine, a plant defence protein with chitinase and lysozyme activity, and its complex with an inhibitor. *Structure* **2**, 1181–1189.
5. Hollis, T., Monzingo, A.F., Bortone, K., Ernst, S., Cox, R. & Robertus, J.D. (2000) The X-ray structure of a chitinase from the pathogenic fungus *Coccidioides immitis*. *Protein Sci.* **9**, 544–551.
6. van Aalten, D.M., Synstad, B., Brurberg, M.B., Hough, E., Riise, B.W., Eijsink, V.G.H. & Wierenga, R.K. (2000) Structure of a two-domain chitotriosidase from *Serratia marcescens* at 1.9-Å resolution. *Proc. Natl Acad. Sci. USA* **97**, 5842–5847.
7. Fusetti, F., von Moeller, H., Houston, D., Rozeboom, H.J., Dijkstra, B.W., Boot, R.G., Aerts, J.M.F.G. & van Aalten, D.M.F. (2002) Structure of human chitotriosidase – Implications for specific inhibitor design and function of mammalian chitinase-like lectins. *J. Biol. Chem.* **277**, 25537–25544.
8. Matsumoto, T., Nonaka, T., Hashimoto, M., Watanabe, T. & Mitsui, Y. (1999) Three-dimensional structure of the catalytic domain of chitinase A1 from *Bacillus circulans* WL-12 at a very high resolution. *Proc. Jpn. Acad., Ser. B, Phys. Biol. Sci.* **75**, 269–274.
9. Terwisscha van Scheltinga, A.C., Hennig, M. & Dijkstra, B.W. (1996) The 1.8 Å resolution structure of hevamine, a plant chitinase/lysozyme, and analysis of the conserved sequence and structure motifs of glycosyl hydrolase family 18. *J. Mol. Biol.* **262**, 243–257.
10. Suzuki, K., Taiyoji, M., Sugawara, N., Nikaidou, N., Henrissat, B. & Watanabe, T. (1999) The third chitinase gene (chiC) of *Serratia marcescens* 2170 and the relationship of its product to other bacterial chitinases. *Biochem. J.* **343**, 587–596.
11. Uchiyama, T., Katouno, F., Nikaidou, N., Nonaka, T., Sugiyama, J. & Watanabe, T. (2001) Roles of the exposed aromatic residues in crystalline chitin hydrolysis by chitinase A from *Serratia marcescens* 2170. *J. Biol. Chem.* **276**, 41343–41349.
12. White, A. & Rose, D.R. (1997) Mechanism of catalysis by retaining beta-glycosyl hydrolases. *Curr. Opin. Struct. Biol.* **7**, 645–651.
13. Davies, G. & Henrissat, B. (1995) Structures and mechanisms of glycosyl hydrolases. *Structure* **3**, 853–859.
14. Vocadlo, D.J., Davies, G.J., Laine, R. & Withers, S.G. (2001) Catalysis by hen egg-white lysozyme proceeds via a covalent intermediate. *Nature* **412**, 835–838.
15. Uitdehaag, J.C.M., Mosi, R., Kalk, K.H., van der Veen, B.A., Dijkhuizen, L., Withers, S.G. & Dijkstra, B.W. (1999) X-ray structures along the reaction pathway of cyclodextrin glycosyltransferase elucidate catalysis in the alpha-amylase family. *Nat. Struct. Biol.* **6**, 432–436.
16. Terwisscha van Scheltinga, A.C., Armand, S., Kalk, K.H., Isogai, A., Henrissat, B. & Dijkstra, B.W. (1995) Stereochemistry of chitin hydrolysis by a plant chitinase/lysozyme and X-ray structure of a complex with allosamidin: evidence for substrate assisted catalysis. *Biochemistry* **34**, 15619–15623.
17. Tews, I., Perrakis, A., Oppenheim, A., Dauter, Z., Wilson, K.S. & Vorgias, C.E. (1996) Bacterial chitobiase structure provides insight into catalytic mechanism and the basis of Tay–Sachs disease. *Nat. Struct. Biol.* **3**, 638–648.
18. Knapp, S., Vocadlo, D., Gao, Z.N., Kirk, B., Lou, J.P. & Withers, S.G. (1996) NAG-thiazoline, an *N*-acetyl-β-hexosaminidase inhibitor that implicates acetamido participation. *J. Am. Chem. Soc.* **118**, 6804–6805.
19. Tews, I., van Scheltinga, A.C.T., Perrakis, A., Wilson, K.S. & Dijkstra, B.W. (1997) Substrate-assisted catalysis unifies two families of chitinolytic enzymes. *J. Am. Chem. Soc.* **119**, 7954–7959.
20. Bokma, E., Rozeboom, H.J., Sibbald, M., Dijkstra, B.W. & Beintema, J.J. (2002) Expression and characterization of active site mutants of hevamine, a chitinase from the rubber tree *Hevea brasiliensis*. *Eur. J. Biochem.* **269**, 893–901.
21. van Aalten, D.M.F., Komander, D., Synstad, B., Gaseidnes, S., Peter, M.G. & Eijsink, V.G.H. (2001) Structural insights into the catalytic mechanism of a family 18 exo-chitinase. *Proc. Natl Acad. Sci. USA* **98**, 8979–8984.
22. Brameld, K.A. & Goddard, W.A. (1998) Substrate distortion to a boat conformation at subsite-1 is critical in the mechanism of family 18 chitinases. *J. Am. Chem. Soc.* **120**, 3571–3580.

23. Papanikolau, Y., Prag, G., Tavlas, G., Vorgias, C.E., Oppenheim, A.B. & Petratos, K. (2001) High resolution structural analyses of mutant chitinase A complexes with substrates provide new insight into the mechanism of catalysis. *Biochemistry* **40**, 11338–11343.
24. Mark, B.L., Vocadlo, D.J., Knapp, S., Triggs-Raine, B.L., Withers, S.G. & James, M.N.G. (2001) Crystallographic evidence for substrate-assisted catalysis in a bacterial β-hexosaminidase. *J. Biol. Chem.* **276**, 10330–10337.
25. Williams, S.J., Mark, B.L., Vocadlo, D.J., James, M.N.G. & Withers, S.G. (2002) Aspartate 313 in the *Streptomyces plicatus* hexosaminidase plays a critical role in substrate-assisted catalysis by orienting the 2-acetamido group and stabilizing the transition state. *J. Biol. Chem.* **277**, 40055–40065.
26. Watanabe, T., Kobori, K., Miyashita, K., Fujii, T., Sakai, H., Uchida, M. & Tanaka, H. (1993) Identification of glutamic acid 204 and aspartic acid 200 in chitinase A1 of *Bacillus circulans* WL-12 as essential residues for chitinase activity. *J. Biol. Chem.* **268**, 18567–18572.
27. Watanabe, T., Uchida, M., Kobori, K. & Tanaka, H. (1994) Site-directed mutagenesis of the Asp-197 and Asp-202 residues in chitinase A1 of *Bacillus circulans* WL-12. *Biosci. Biotechnol. Biochem.* **58**, 2283–2285.
28. Tsujibo, H., Orikoshi, H., Imada, C., Okami, Y., Miyamoto, K. & Inamori, Y. (1993) Site-directed mutagenesis of chitinase from *Alteromonas* sp. strain O-7. *Biosci. Biotechnol. Biochem.* **57**, 1396–1397.
29. Lin, F.P., Chen, H.C. & Lin, C.S. (1999) Site-directed mutagenesis of Asp313, Glu315, and Asp391 residues in chitinase of *Aeromonas caviae*. *IUBMB Life* **48**, 199–204.
30. Lu, Y., Zen, K.C., Muthukrishnan, S. & Kramer, K.J. (2002) Site-directed mutagenesis and functional analysis of active site acidic amino acid residues D142, D144 and E146 in *Manduca sexta* (tobacco hornworm) chitinase. *Insect Biochem.* **32**, 1369–1382.
31. Kolstad, G., Synstad, B., Eijsink, V.G.H. & van Aalten, D.M. (2002) Structure of the D140N mutant of chitinase B from *Serratia marcescens* at 1.45 Å resolution. *Acta Crystallogr. D. Biol. Crystallogr.* **58**, 377–379.
32. Houston, D.R., Shiomi, K., Arai, N., Omura, S., Peter, M.G., Turberg, A., Synstad, B., Eijsink, V.G.H. & van Aalten, D.M. (2002) High-resolution structures of a chitinase complexed with natural product cyclopentapeptide inhibitors: mimicry of carbohydrate substrate. *Proc. Natl Acad. Sci. USA.* **99**, 9127–9132.
33. Nielsen, J.E., Andersen, K.V., Honig, B., Hooft, R.W., Klebe, G., Vriend, G. & Wade, R.C. (1999) Improving macromolecular electrostatics calculations. *Protein Eng.* **12**, 657–662.
34. Nielsen, J.E. & McCammon, J.A. (2003) On the evaluation and optimization of protein X-ray structures for pKa calculations. *Protein Sci.* **12**, 313–326.
35. Brurberg, M.B., Nes, I.F. & Eijsink, V.G.H. (1996) Comparative studies of chitinases A and B from *Serratia marcescens*. *Microbiology* **142**, 1581–1589.
36. Stoll, V.S. & Blanchard, J.S. (1990) Buffers – Principles and Practice. *Methods Enzymol.* **182**, 24–38.
37. Vriend, G. (1990) WHAT IF: a molecular modeling and drug design program. *J. Mol. Graph.* **8**, 52–56.
38. Nielsen, J.E. & Vriend, G. (2001) Optimizing the hydrogen-bond network in Poisson–Boltzmann equation-based pK(a) calculations. *Proteins* **43**, 403–412.
39. Nielsen, J.E. & McCammon, J.A. (2003) Calculating pKa values in enzyme active sites. *Protein Sci.* **12**, 1894–1901.
40. Chinea, G., Padron, G., Hooft, R.W.W., Sander, C. & Vriend, G. (1995) The use of position-specific rotamers in model-building by homology. *Proteins: Struct. Funct. Genet.* **23**, 415–421.
41. DeLano, W.L. (2002) *The PyMOL Molecular Graphics System*. DeLano Scientific, San Carlos, CA, USA. http://www.pymol.org
42. Joshi, M.D., Sidhu, G., Nielsen, J.E., Brayer, G.D., Withers, S.G. & McIntosh, L.P. (2001) Dissecting the electrostatic interactions and pH-dependent activity of a family 11 glycosidase. *Biochemistry* **40**, 10115–10139.
43. Kyte, J. (1995) *Mechanism in Protein Chemistry*. Garland Publishing, Inc., New York.
44. Papanikolau, Y., Tavlas, G., Vorgias, C.E. & Petratos, K. (2003) De novo purification scheme and crystallization conditions yield high-resolution structures of chitinase A and its complex with the inhibitor allosamidin. *Acta Crystallogr. D. Biol. Crystallogr.* **59**, 400–403.
45. Bortone, K., Monzingo, A.F., Ernst, S. & Robertus, J.D. (2002) The structure of an allosamidin complex with the *Coccidioides immitis* chitinase defines a role for a second acid residue in substrate-assisted mechanism. *J. Mol. Biol.* **320**, 293–302.
46. Subroto, T., van Koningsveld, G.A., Schreuder, H.A., Soedjanaatmadja, U.M. & Beintema, J.J. (1996) Chitinase and β-1,3-glucanase in the lutoid-body fraction of *Hevea* latex. *Phytochemistry* **43**, 29–37.
47. McIntosh, L.P., Hand, G., Johnson, P.E., Joshi, M.D., Korner, M., Plesniak, L.A., Ziser, L., Wakarchuk, W.W. & Withers, S.G. (1996) The pKa of the general acid/base carboxyl group of a glycosidase cycles during catalysis: a 13C-NMR study of *Bacillus circulans* xylanase. *Biochemistry* **35**, 9958–9966.
48. Joshi, M.D., Sidhu, G., Pot, I., Brayer, G.D., Withers, S.G. & McIntosh, L.P. (2000) Hydrogen bonding and catalysis: a novel explanation for how a single amino acid substitution can change the pH optimum of a glycosidase. *J. Mol. Biol.* **299**, 255–279.